# DEVELOPING COMPRESSIBLE TURBULENT FLOW AND HEAT TRANSFER IN CIRCULAR TUBE WITH UNIFORM INJECTION OR SUCTION

**Asst.Prof.Dr.Ihsan Y.Hussain**
**Mech.Engr.Dept.**
**College of Engineering**
**University of Baghdad**
**Baghdad-Iraq**

**Ayad M. Salman**
**Mechanical Engineer**
**Energy & Fuel Research Center**
**University of Technology**
**Baghdad-Iraq**

**Adil A. Mohammed**
**Mechanical Engineer**
**Baghdad-Iraq**
**Adekef@yahoo.Com**

## ABSTRACT

In the present work , a numerical study has been made for the developing compressible turbulent flow and heat transfer in circular tube with uniform injection or suction. The study included the numerical solution of the continuity, momentum and energy equations together with the two equations of the (k-**ε**) turbulence model, by using the Finite Difference Method (FDM). The air was used as the working fluid, and the circular passage was composed of tube with diameter (20.0) cm , and the length was 130 (hydraulic diameter) .The Reynolds number of the flow was ($Re=1.78x10^6$), and the Mach number (M=0.44) the ratio of the transverse velocity at the wall ($v_w$) to the axial velocity at inlet ($U_{in}$), $\Omega=(v_w/U_{in})$, for suction equal(0.001) and for injection (-0.001).. The wall of the tube was heated with constant wall temperature ($T_w$) and in other case with constant heat flux ($Q_w$) as a thermal boundary condition. The development of both hydrodynamic and thermal boundary layers occurs simultaneously. The computational algorithm is capable of calculating the hydrodynamic parameters such as the velocities , friction factor , turbulence structure which includes the Reynolds stress and the turbulent kinetic energy and eddy viscosity. Besides, the thermal parameters are also predicted, such as the temperature, Nusselt number, and the turbulent heat fluxes.The Results showed that the hydrodynamic and thermal entrance length is increased with the increasing of Reynolds number. The suction caused a flatten for the velocity profile and thus decreasing the hydrodynamic entrance length, and caused an increase in the Nusselt number and decreasing the local coefficient of friction, but injection caused a steeping of the velocity profile , and thus increasing the entrance hydrodynamic length and caused a decrease in the Nusselt number and increase the local coefficient of friction. Turbulent kinetic energy and turbulent heat flux are decreased with

suction and increased with injection .Predictions have been obtained which are in good agreement with results obtained by past experimental and theoretical work.

**الخلاصة**

**يتضمن البحث الحالي دراسة نظرية عددية للجريان المضطرب الأنضغاطي غير تام التطور مع انتقال الحرارة خلال مجرى أنبوبي مع حالة حقن أو سحب باستخدام طريقة الحل العددي لمعادلات الاستمرارية والزخم والطاقة مع معادلتي نموذج الاضطراب (k-ε) باستخدام طريقة الفروق المحددة (FDM) ، الحسابات العددية منفذة باستخدام الهواء كمائع عمل يمر خلال مجرى أنبوبي قطره (20) سم وطوله يساوي (130) قطر هايدروليكي، رقم رينولد للهواء يساوي ($1.78x10^6$) وبرقم ماخ يساوي (M=0.44)، تم تسخين جدار الأسطوانة باستخدام شرط درجة حرارة الجدار ثابتة مرة وأخرى باستخدام شرط فيض حراري ثابت كذلك استخدم مرور الهواء عبر الجدار ($v_w$) باتجاهين كشرطين حديين وبنسبة $\Omega$ =($v_w/U_{in}$), الأول في حالة خروج الهواء من الأنبوب ( امتصاص ) وكانت النسبة (0.001) والأخرى دخول الهواء إلى الأنبوب ( حقن ) وكانت النسبة (0.001-) . تحدث عملية التطور الهيدروديناميكي والحراري آنيا" . أمكانية الحل العددي تتضمن حساب الصفات الهيدروديناميكية مثل مركبات منحنيات السرعة ومعامل الاحتكاك ، هيكل الاضطراب مثل منحنيات إجهاد رينولدز والطاقة الحركية المضطربة واللزوجة الدوامية ، كذلك تم حساب الصفات الحرارية مثل توزيع درجات ورقم نسلت والفيض الحراري المضطرب لمنطقة الحساب . بينت النتائج زيادة طول الدخول الهيدروديناميكي والحراري بزيادة رقم رينولدز ، كما بينت أن حالة الامتصاص تسبب استواء منحنى السرعة وقصر طول الدخول الهيدروديناميكي وزيادة رقم نسلت كما يسبب نقصان معامل الاحتكاك الموضعي والعكس فأن الحقن يؤدي إلى تحدب منحنى السرعة وزيادة طول الدخول الهيدروديناميكي وانخفاض رقم نسلت مع نقصان في قيمة معامل الاحتكاك الموضعي . الطاقة الحركية المضطربة والفيض الحراري المضطرب يقلان خلال عملية الامتصاص بينما يزيدان خلال عملية الحقن. لتأكيد النتائج العددية فقد تم مقارنتها مع نتائج البحوث السابقة وكان التوافق بين النتائج جيداً ويؤكد موثوقية الخطوات العددية المقترحة في حسابات الجريان المضطرب وانتقال الحرارة خلال المجرى الأنبوبي .**

**KEY WORDS: Flow and Heat Transfer, Developing, Compressible, Turbulent , Injection and Suction, Circular Tube.**

## INTRODUCTION

The behavior of fluid flow over the surface of a porous material with mass transfer at the boundary is encountered in a wide range of applications such as, aerodynamic boundary layer control, wall suction to delay separation and transition from laminar to turbulent flow, transpiration or sweat cooling of heated surfaces, which is applied to gas turbine blades, ram-jet intakes, rocket walls, combustion chamber walls exposed to high temperature gases, and so on. In this cooling method, cooling is forced through a porous wall and injected into the high

temperature stream. In this way the wall temperature is reduced by forming a heat insulating layer between the hot air and the wall. In addition, heat is removed from the wall by the cooling fluid passing through the interstices. The control of the establishment length in the inlet region of a channel. It is found that the injection of fluid increases the rate of growth of the boundary layer .The characteristics of flow with condensation are analogous in many respects to the flow of fluid over a porous surface with mass transfer at the wall. **(Hasan , 1984).** For internal flow through channels with porous walls (suction or injection), there exists many applications such as in the fields of transpiration cooling, gaseous diffusion, boundary-layer control and ultrahigh filtration. As an effective boundary layer control method, fluid flow in channels or pipes with fluid suction or injection through the wall surface was first investigated by mechanical engineers as early as 1904. Early researchers only focused on fluid flow past a flat surface suction or injection in a part of the whole surface, it was, assumed that the quantity of fluid removed from the stream by suction , so small that only fluid particles in the immediate neighborhood of the wall were suked away, this was equivalent to saying that the ratio of suction velocity to free stream velocity ($\Omega$) was very small , say ($\Omega$ =0.0001 to 0.01) , the condition of no slip at the wall is retained with suction present, as well as, the expression for shearing stress at the wall. **(Schilichting , 2000 )**.

The present work investigates the effects of injection or suction on the development of compressible and turbulent flow and heat transfer through circular tube. The governing continuity , momentum and energy equations are solved numerically by using Finite Difference Method (FDM). The simultaneous development of both hydrodynamic and thermal boundary layers will be considered with uniform injection or suction through the wall.

## GOVERNING EQUATIONS

Steady state, two dimensional axis-Symmetric , compressible , developing turbulent flow(both hydrodynamically and thermally), with uniform injection or suction, and negligible thermal dissipation and body forces and axial diffusion effects will be assumed.

Accordigly the governing, continuity , momentum and energy conservation , kinetic energy of turbulence (k) and viscous will be as follows :-

Continuity Equation.

$$\frac{\partial(\rho u)}{\partial z}+\frac{1}{r}\frac{\partial(\rho v)}{\partial r}=0 \qquad (1)$$

Momentum equation in radial direction ;

$$\rho\left(v\frac{\partial v}{\partial r}+u\frac{\partial v}{\partial z}\right)=-\frac{\partial p}{\partial r}+\left[\frac{1}{r^2}\frac{\partial}{\partial r}\left\{r^3\mu_{eff}\frac{\partial}{\partial r}\left(\frac{v}{r}\right)\right\}\right]+\frac{\partial}{\partial z}\left(\mu_{eff}\frac{\partial v}{\partial z}\right)+s_r \qquad (2)$$

Where ; $$s_r=\frac{1}{r^2}\frac{\partial}{\partial r}\left\{r^3\mu_t\frac{\partial}{\partial r}\left(\frac{v}{r}\right)\right\}+\frac{\partial}{\partial z}\left(\mu_t\frac{\partial u}{\partial r}\right)-\frac{2}{3}\rho\frac{\partial k}{\partial r}$$

Momentum equation in axial direction ;

$$\rho\left(v\frac{\partial u}{\partial r}+u\frac{\partial u}{\partial z}\right)=-\frac{\partial p}{\partial z}+\left[\frac{1}{r}\frac{\partial}{\partial r}\left\{r\mu_{eff}\frac{\partial u}{\partial r}\right\}\right]+\frac{\partial}{\partial z}\left(\mu_{eff}\frac{\partial u}{\partial z}\right)+s_z \quad (3)$$

Where; $s_z=\frac{1}{r}\frac{\partial}{\partial r}\left\{r\mu_t\frac{\partial v}{\partial z}\right\}+\frac{\partial}{\partial z}\left(\mu_t\frac{\partial u}{\partial z}\right)-,\frac{2}{3}\rho\frac{\partial k}{\partial z}$ $\qquad \mu_{eff}=\mu+\mu_t$

Energy equation

$$\rho\left(v\frac{\partial T}{\partial r}+u\frac{\partial T}{\partial z}\right)=\frac{1}{r}\frac{\partial}{\partial r}\left(r\frac{\mu_{eff}}{\mathrm{Pr}_{eff}}\frac{\partial T}{\partial r}\right)+\frac{\partial}{\partial z}\frac{\mu_{eff}}{\mathrm{Pr}_{eff}}\frac{\partial T}{\partial z} \quad (4)$$

Equation of state (Perfect gas) ;

$$P=\rho\Re T \quad (5)$$

Sutherlands law of viscosity

$$\frac{\mu}{\mu_0}=\left(\frac{T}{T_0}\right)^{3/2}\left(\frac{T_0+S}{T+S}\right) \quad (6)$$

Where; $T_0$ =273.16 , $\mu_0$ =1.708x10 kg/m.sec , S=110 .

(k-ε) Model ;

Kinetic energy (k) equation :-

$$\rho\left(v\frac{\partial k}{\partial r}+u\frac{\partial k}{\partial z}\right)=\frac{1}{r}\frac{\partial}{\partial r}\left(r\frac{\mu_t}{\sigma_k}\frac{\partial k}{\partial r}\right)+\frac{\partial}{\partial z}\left(\frac{\mu_t}{\sigma_k}\frac{\partial k}{\partial z}\right)+G-\rho\varepsilon \quad (7)$$

Viscous dissipation (ε) equation :-

$$\rho\left(v\frac{\partial \varepsilon}{\partial r}+u\frac{\partial \varepsilon}{\partial z}\right)=\frac{1}{r}\frac{\partial}{\partial r}\left(r\frac{\mu_t}{\sigma_\varepsilon}\frac{\partial \varepsilon}{\partial r}\right)+\frac{\partial}{\partial z}\left(\frac{\mu_t}{\sigma_\varepsilon}\frac{\partial \varepsilon}{\partial z}\right)+C_{\varepsilon 1}\frac{\varepsilon}{k}G-C_{\varepsilon 2}\rho\frac{\varepsilon^2}{k} \quad (8)$$

$$G=\mu_t\left[2\left\{\left(\frac{\partial v}{\partial r}\right)^2+\left(\frac{\partial u}{\partial z}\right)^2\right\}+\left(\frac{\partial v}{\partial z}+\frac{\partial u}{\partial r}\right)^2\right] \quad (9)$$

Boundary Conditions ;

Entrance condition

$u=U_{in}$ , $v=0$ , $t=T_{in}$ (10)

$$k_{in}=C_k U_{in}^2 \qquad \varepsilon_{in}=C_\mu\, k_{in}^{\frac{3}{2}}\Big/\left(0.5D_h C_\varepsilon\right)$$

, (11)

$C_\varepsilon$ =0.03 , $C_k$=0.003 , $D_h$ = (12)

Exit Condition

$$(13)\ \frac{\partial u}{\partial z}=\frac{\partial k}{\partial z}=\frac{\partial \varepsilon}{\partial z}=0 \quad , \quad \frac{\partial T}{\partial z}=Constant$$

Wall and Center line Conditions

u(R,z)=0 , v(R,z)=$v_w$ (14)

$\Omega = v_w / U_{in}$ (15)

For the center line:-

$\frac{\partial u}{\partial r}$(0,z)=0 , v(0,z)=0 (16)

Temperature boundary condition:-

$T(R,z)=T_w$ (constant wall temperature) (17)

$$\lambda\frac{\partial T}{\partial r}(R,z)=Q_w \quad \text{( constant wall heat flux )} \qquad (18)$$

Flow Through Porous Wall

$$\Omega=\frac{V_w}{U_{in}} \qquad (20)$$

$$\Psi=\frac{\dot{m}_{wall}}{\dot{m}}=\frac{\rho\pi DLV_w}{\rho\frac{\pi D^2}{4}U_{in}}=4\frac{V_w}{U_{in}}\frac{L}{D} \qquad (21)$$

$$\Psi=4\Omega Z^* \qquad (22)$$

**NUMERICAL SOLUTION.**

The governing equations will be solved numerically by using (Explicit Finite Differences Method) **(Ayad, 2003)**, the node – point has subscripts ( i , j ) denoting cylindrical coordinate in ( r , z ) directions. The coordinates for each node are (r=iΔr), (z=jΔz) .

The convection terms of the axial momentum equation will be changed to finite differences by using back-ward differences. The pressure gradient will be changed to algebraic term by

using (Upwind Differences). For the (Diffusion Terms) in the right side of the equation, the (Central Differences ) will be used . The following final form is obtained :-

$$a_1 u_{(i,j)} = a_2 u_{(i+1,j)} + a_3 u_{(i,j+1)} + a_4 u_{(i-1,j)} + a_5 u_{(i,j-1)} - \frac{p_j - p_{(j-1)}}{\Delta z} + Su \qquad (23)$$

where :-

$$a_1 = \frac{\rho_{(i,j)} v_{(i,j)}}{\Delta r} + \frac{\rho_{(i,j)} u_{(i,j)}}{\Delta z} + \frac{r_{(i+0.5,j)} \mu_{eff(i+0.5,j)}}{r_{(i,j)} (\Delta r)^2} + \frac{r_{(i-0.5,j)} \mu_{eff(i-0.5,j)}}{r_{(i,j)} (\Delta r)^2} + \frac{\mu_{eff(i,j+0.5)}}{(\Delta z)^2} + \frac{\mu_{eff(i,j-0.5)}}{(\Delta z)^2} + \frac{\mu_{t(i,j+0.5)}}{(\Delta z)^2} + \frac{\mu_{t(i,j-0.5)}}{(\Delta z)^2}$$

$$a_2 = \frac{r_{(i+0.5,j)} \mu_{eff(i+0.5,j)}}{r_{(i,j)} \Delta r^2}, \; a_3 = \frac{\mu_{eff(i,j+0.5)} + \mu_{t(i,j+0.5)}}{\Delta z^2}, \; a_4 = \frac{r_{(i-0.5,j)} \mu_{eff(i-0.5,j)}}{r_{(i,j)} \Delta r^2}$$

$$a_5 = \frac{\rho_{(i,j)} u_{(i,j)}}{\Delta z} + \frac{\mu_{eff(i,j-0.5)} + \mu_{t(i,j-0.5)}}{\Delta z^2}$$

$$Su = \frac{r_{(i+1,j)} \mu_{t_{(i+1,j)}}}{4 r_{(i,j)} \Delta r \Delta z} v_{(i+1,j+1)} - \frac{r_{(i-1,j)} \mu_{t_{(i-1,j)}}}{4 r_{(i,j)} \Delta r \Delta z} v_{(i-1,j+1)} - \frac{r_{(i+1,j)} \mu_{t_{(i+1,j)}}}{4 r_{(i,j)} \Delta r \Delta z} v_{(i+1,j-1)} + \frac{r_{(i-1,j)} \mu_{(i-1,j)}}{4 r_{(i,j)} \Delta r \Delta z} v_{(i-1,j-1)} - \frac{1}{3} \frac{\rho_{(i,j+1)} \kappa_{(i,j+1)} - \rho_{(i,j)} \kappa_{(i,j-1)}}{\Delta z}$$

The mass balance equation for a typical control volume gives ;

$$\dot{m}_{in} + \dot{m}_{wall} = m \qquad (24)$$

$$\dot{m}_{in} = \int_0^R 2\pi \rho_{(i,j)} u_{(i,j)} r dr \qquad (25)$$

$$\dot{m} = \int_0^R 2\pi \rho_{(i,j)} u_{(i,j)} r dr \pm 4\Omega \Psi Z^* \qquad (26)$$

The (+ve) sign in equation (26) is for suction and the (-ve) sign is for injection. The mean pressure difference ( $\overline{p}_j - \overline{p}_{(j-1)}$ ) in equation (23) can be calculated by ( mass conservation ) **(Caretto & et.al,1972)** as :-

$$\overline{p}_j = \overline{p}_{(j-1)} + \frac{\dot{m} - 2\pi \rho_{(i,j)} \int_0^R \alpha_{(i,j)} r dr}{2\pi \rho_{(i,j)} \int_0^R \beta r dr} \qquad (27)$$

The continuity equation is converted to algebraic form by using the (Back Ward Differences), the following final form is obtained:-

$$v_{(i,j)} = \frac{r_{(i-1,j)}\rho_{(i-1,j)}}{r_{(i+1,j)}\rho_{(i,j)}} v_{(i-1,j)} + \frac{\Delta r}{\Delta z} \frac{r_{(i,j)}}{\rho_{(i,j)} r_{(i+1,j)}} (\rho_{(i,j-1)} u_{(i,j-1)} - \rho_{(i,j)} u_{(i,j)}) \quad (28)$$

To convert the two equations for (k-ε) model to the numerical form we use the (Backward Differences) for the convective term and the (Central Differences) for diffusion term , the result is ;

$$c_1 k_{(i,j)} = c_2 k_{(i+1,j)} + c_3 k_{(i,j+1)} + c_4 k_{(i-1,j)} + c_5 k_{(i,j-1)} + S_k \quad (29)$$

Where ;

$$c_1 = \frac{\rho_{(i,j)} v_{(i,j)}}{\Delta r} + \frac{\rho_{(i,j)} u_{(i,j)}}{\Delta z} + \frac{r_{(i+0.5,j)}\mu_{t_{(i+0.5,j)}} + r_{(i-0.5,j)}\mu_{t_{(i-0.5,j)}}}{r_{(i,j)}\sigma_k (\Delta r)^2} + \frac{\mu_{t_{(i,j+0.5)}} + \mu_{t_{(i,j-0.5)}}}{\sigma_k (\Delta z)^2}$$

$$c_2 = \frac{r_{(i+0.5,j)}\mu_{t_{(i+0.5,j)}}}{r_{(i,j)}\sigma_k (\Delta r)^2},\ c_3 = \frac{\mu_{t_{(i,j+0.5)}}}{\sigma_k (\Delta z)^2},\ c_4 = \frac{\rho_{(i,j)} v_{(i,j)}}{\Delta r} + \frac{r_{(i-0.5,j)}\mu_{t_{(i-0.5,j)}}}{r_{(i,j)}\sigma_k (\Delta r)^2}$$

$$c_5 = \frac{\rho_{(i,j)} u_{(i,j)}}{\Delta z} + \frac{\mu_{t_{(i,j-0.5)}}}{\sigma_k (\Delta z)^2},\ S_k = G_{(i,j)} - \rho_{(i,j)} \varepsilon_{(i,j)}$$

Dissipation energy (ε) equation.

$$d_1 \varepsilon_{(i,j)} = d_2 \varepsilon_{(i+1,j)} + d_3 \varepsilon_{(i,j+1)} + d_4 \varepsilon_{(i-1,j)} + d_5 \varepsilon_{(i,j-1)} + S_\varepsilon \quad (30)$$

define the following coefficient:-

$$d_1 = \frac{\rho_{(i,j)} v_{(i,j)}}{\Delta r} + \frac{\rho_{(i,j)} u_{(i,j)}}{\Delta z} + \frac{r_{(i+0.5,j)}\mu_{t_{(i+0.5,j)}} + r_{(i-0.5,j)}\mu_{t_{(i-0.5,j)}}}{r_{(i,j)}\sigma_\varepsilon (\Delta r)^2} + \frac{\mu_{t_{(i,j+0.5)}} + \mu_{t_{(i,j-0.5)}}}{\sigma_\varepsilon (\Delta z)^2} + \frac{C_{\varepsilon 2}\rho_{(i,j)}\varepsilon_{(i,j)}}{k_{(i,j)}}$$

$$d_2 = \frac{r_{(i+0.5,j)}\mu_{t_{(i+0.5,j)}}}{r_{(i,j)}\sigma_\varepsilon (\Delta r)^2},\ d_3 = \frac{\mu_{t_{(i,j+0.5)}}}{\sigma_\varepsilon (\Delta z)^2},\ d_4 = \frac{\rho_{(i,j)} v_{(i,j)}}{\Delta r} + \frac{r_{(i-0.5,j)}\mu_{t_{(i-0.5,j)}}}{r_{(i,j)}\sigma_\varepsilon (\Delta r)^2}$$

$$d_5 = \frac{\rho_{(i,j)} u_{(i,j)}}{\Delta z} + \frac{\mu_{t_{(i,j-0.5)}}}{\sigma_\varepsilon (\Delta z)^2},\ S_\varepsilon = \frac{C_{\varepsilon 1} G_{(i,j)} \varepsilon_{(i,j)}}{k_{(i,j)}}\ .$$

The energy equation can be converted to algebraic form by using the (Backward Differences) for the diffusion term and (Central Differences) for the convective term , the following linear equation is obtained:-

$$e_1 T_{(i,j)} = e_2 T_{(i+1,j)} + e_3 T_{(i,j+1)} + e_4 T_{(i-1,j)} + e_5 T_{(i,j-1)} \qquad (31)$$

Where ;

$$e_1 = \frac{\rho_{(i,j)} v_{(i,j)}}{\Delta r} + \frac{\rho_{(i,j)} u_{(i,j)}}{\Delta z} + \frac{r_{(i+0.5,j)} \mu_{(i+0.5,j)} + r_{(i-0.5,j)} \mu_{eff(i-0.5,j)}}{r_{(i,j)} p_r (\Delta r)^2} + \frac{\mu_{eff(i,j+0.5)} + \mu_{eff(i,j-0.5)}}{p_{r_{eff}} (\Delta z)^2}$$

$$e_2 = \frac{r_{(i+0.5,j)} \mu_{eff(i+0.5,j)}}{r_{(i,j)} p_{r_{eff}} (\Delta r)^2}, e_3 = \frac{\mu_{eff(i,j+0.5)}}{p_{r_{eff}} (\Delta z)^2}, e_4 = \frac{\rho_{(i,j)} v_{(i,j)}}{\Delta r} + \frac{r_{(i+0.5,j)} \mu_{eff(i-0.5,j)}}{r_{(i,j)} (\Delta r)^2 p_{r_{eff}}}$$

A numerical calculations algorithm was developed to solve the above equations numerically, and a computer program was built to implement this algorithm.

## RESULTS AND DISCUSSION

The results of the developed computational algorithm for turbulent flow of air through a porous circular tube will be discussed for the following case:-

$P_{in}$ = 1 bar, $T_{in}$ = 100 $^oC$, $T_w$ = 100 $^oC$, $Q_w$=1000w/$m^2$, $U_{in}$= (90-150) m/s, Re= 1.78 x$10^7$, M = 0.26 – 0.44, $Z^*$ = 130.

The grid size was taken as, (m=500) in axial direction and (n=20) in radial direction.

**Fig.1** shows the development of the boundary layer for flow in solid wall with ( Re=1.78x$10^6$) at ($Q_w$=1000w/$m^2$). Near the wall, the viscous effects are dominant, so the boundary layer grows in the flow (axial) direction until it reaches apposition ,after that the boundary shape fixed, this mean that flow is fully developed. It can be concluded that the hydrodynamic entrance length is equal to (140) pipe diameter approximately. **Fig.2** shows the radial distribution for the axial velocity profile at constant wall temperature and constant heat flux. **Fig.3** show the effect of Reynolds number on the development of velocity profiles at constant wall temperature and constant heat flux , it is that the velocity increased with the increasing of Reynolds number, the same result is obtained by **(Ayad,2003)**. **Fig.4** shows the dimensionless axial velocity development for various dimensionless radial positions, with constant wall temperature and constant heat flux, the same result is obtained by **(Stephenson,1976)**.

**Fig.5** shows the effect of suction and injection on the velocity profiles at constant wall temperature first and constant heat flux second, the velocity profile is flattened at suction and became steeper at injection, the same result is obtained by **(Hasan,1984)**. With the presence of mass transfer through perforations, the velocity profile is altered due to the interaction between the axial flow and the perforation flow, for the injection case, the injection lifts and expands the turbulent boundary layer and thus increases the axial velocity beyond the layer while decreases the velocity within the layer to follow the mass conservation law. As a consequence the axial velocity near the pipe wall decreases and on the contrary, the suction lowers and reduces the boundary layer and thus decreases the velocity outside the layer but increases the velocity inside the layer, and results in an increase of the axial velocity near the pipe wall analysis, this is consistent with the numerical observations of **(Kinney & Sparrow,1970)** for pipe flow with suction through the pipe wall.For suction and injection $\Omega$(+0.001, -0.001) the

hydrodynamic length from the entrance to the fully developed velocity profile for the solid wall at constant wall temperature is equal to (130) diameters , decreases to (120) diameters , but for injection increases to (140) diameters, approximately. For Constant heat flux the hydrodynamic length for the solid wall is equal to (140) diameters , for suction decreased to (130) diameters , and for injection increased to (150) diameters ,approximately.

**Fig.6** shows the development of turbulent kinetic energy ($2k/u_b^2$)with constant wall temperature , and constant heat flux , notice that the maximum value of the kinetic energy is in the region near the wall , and decreases in turbulent kinetic energy value with the increasing of Reynolds number because the axial velocity profile decreases with the increasing of the Reynolds number , also the hydrodynamic entry length ,at which the turbulent kinetic energy is fully developed , increases with the increasing of the Reynolds number. Fig (9) shows the effect of suction and injection on the turbulent kinetic energy ,turbulent kinetic energy increased with injection and decreased with suction, the same result is obtained by **(Ayad,2003)**.

**Fig.7** shows the three dimensional development of the turbulent viscosity with. The turbulent viscosity increases with the increasing of the Reynolds number , so increasing the length needed for the fully developed profile, the same result is obtained by **(Ayad,2003)**.

**Fig.8** show the development of air density for Reynolds number at constant wall temperature and constant heat flux , notice that for constant wall temperature the density stay constant near the wall but for constant heat flux decreases because of the increasing of the wall temperature down stream , the same result is obtained by **(Ayad,2003)**, suction increases the density and injection decreases it.

**Fig.9** shows the steps of developing Reynolds Stress . Find that the Reynolds Stress equal to zero at maximum velocity near the center line and the maximum value is in the region near the wall, the same result is obtained by **(Ayad,2003)**. Show that the suction causes to flatten the velocity profile then decreases the Reynolds stress but the injection which causes to steeper the velocity profile then decreases the Reynolds stress.

**Fig.10** shows the development of the local coefficient of friction , it decreases with the increasing of the Reynolds number because the boundary layer decreases , and the turbulent kinetic energy that enter in calculating the shear stress which can be calculated from the wall function decreases too. **Fig.11** shows the effect of suction and injection, the local coefficient of friction decreases with the suction because that the boundary layer decreases with the suction case so the turbulent kinetic energy decreases , but in the injection case the local coefficient of friction increases because the boundary layer increases , the same result is obtained by **(Moshe,1986)**.

**Fig.12** shows development of the isothermal lines, notice that the temperature increases along side with axial flow direction and decrease with radial direction .**Fig.13-a** shows the effect of Reynolds number on the overall heating of the flow. **Fig.13-b** shows the effect of Reynolds Number on the wall temperature. The overall heating of the flow and the wall temperature increase parabolic in the developing region, and decrease with the increasing of Reynolds number, the same result is obtained by **(Ayad,2003)**.

**Fig.15** shows the radial distribution of the turbulent heat flux at many positions , the turbulent heat flux values is the maximum near the wall and in the fully developed region

because of the high temperature of the heated wall and there is a decreasing toward the center line because of the difference in the temperature between the wall and the fluid **,** the same result is obtained by **(Ayad,2003)** .

**Fig.16** shows the axial distribution of the Nusselts number at constant wall temperature and constant heat flux, the maximum value at the entrance region because the thermal boundary layer thickness equal to zero and the heat transfer coefficient by convection is maximuim, after that the thermal boundary layer grows and the coefficient of heat transfer decreases and so the Nusselt number decreases gradually until it reaches constant value , it needs longer length , also for the same reason the Nusselts number increases with the increasing of the Reynolds number for constant wall temperature and constant heat flux, the same result is obtained by **(Ayad,2003)** . **Fig.17** shows the effect of suction and injection on Nusselts number, suction increases the value of Nusselt Number, the same result is obtained by **(Aggarwal & Hollingsworth,1973)** and injection decreases it. **Fig,18** shows the radial temperature development profile at constant wall temperature and constant heat flux . **Fig.19** shows the relation between mean Nusselt Number and Rynolds Number, increasing the Rynolds Number causes significantly increased heat transfer, so increasing Re causing an increase in $Nu_{mean}$ , the same result is obtained by **(Hasan,1984)**.

**Comparison of the Results** .

**Fig.20-a** shows the comparison of the velocity profile for the present work which is calculated theoretically with experimental results of **(Aggarwal et al,1972)**, which was done on a porous tube with internal diameter (D=0.02565 m) and length (L=0.2465)m, for Reynolds Number Re(101160) and $Z^*$ =9.3 with rate of suction $\Omega$ =(0.0135 ) . **Fig.20-b** shows the comparison of the development of the profile , at (Re=338000) for the present work with the results of the theoretical work which was done by **(Stephenson,1976)** , on a tube with (D=0.2 m) with (Re=388000) at
$Z^*$ =(0.0 , 0.75, 0.94).

**CONCLUSIONS.**

The numerical results of the present work show that, the velocity profile, was flattened with suction and steepened with injection, its value was decreased with the increasing of Reynolds number and with suction .The hydrodynamic length, from the entrance to the fully developed region, was increased with the increasing of Reynolds number and with suction, it was decreased with injection. Turbulent kinetic energy was decreased in the region far from the wall and by suction, and it was increased by injection. Reynolds stress was vanished far from the wall; it was increased by injection and decreased by suction. Local coefficient of friction was decreased with suction and with the increasing of Reynolds number, it was increased with injection. Turbulent heat flux for constant wall temperature and constant heat flux has a maximum value near the wall and minimum value in the center line. Decreasing of the wall temperature at constant heat flux and the bulk temperature increases with injection and decrease with suction. Nusselts number was increased with the Reynolds number and with suction, and it was decreased with injection.

## REFERENCES

Aggarwal,J.K,(1973) " Heat Transfer for Turbulent flow with Suction in a Porous Tube " J. Heat Mass Transfer , Vol.16.pp.591-609, 1973.

Aggarwal,J.K., Hollingsworth,M.A and Mayhew,Y.R , (1972) " Experimental Friction Factors for Turbulent Flow with Suction in a Porous Tube " J. Heat Mass Transfer. Vol.15.pp.1585-1602, 1972 .

Ayad Mahmoud Salman , (2003) , " Turbulent Forced Convection Heat Transfer in the Developing Flow Through Concentric Annuli " Msc. thesis , Mechanical Engineering Department . University of Technology.

Caretto,L.S., Curr,R.M and Spalding,D.B, (1972), "Two Numerical Methods For Three-Dimensional Boundary Layers," Compt. Meth. Appl. Mech. Engng., Vol. 1, PP. 39-57.

Hasan Abdul – Aziz Hasan , (1984) , " Length to Diameter Ratio Effects on Friction and Heat Transfer of Turbulent Flow in a Porous Tube " Ph.D. thesis , Mech. Eng. Dept., University of Bristol.

Kenny,R.B and Sparrow,E.M , (1970) " Turbulent Flow , Heat Transfer , and Mass transfer in a Tube with Surface Suction " ASME J. of Heat Transfer, PP.117-125 , February 1970 .

Moshe Ben-Reuven , (1984) " The Viscous Wall-Layer Effect in Injected Porous Pipe Flow " AIAA Journal , Vol.24.pp.284-294,1984.

Schlichting,H, (2000), "Boundary Layer Theory,"McGraw-Hill, New York.

Stephenson,P.L , (1976) , " A Theoretical Study of Heat Transfer in Two-Dimensional Turbulent Flow in a Circular Pipe and Between Parallel and Diverging Plates " J. Heat Mass Transfer , Vol.19.pp.413-423, 1976.

## NOMENCLATURE

LATIN SYMBOLS

| | | |
|---|---|---|
| $C_f$ | Local coefficient of friction ( = $\tau_w / 0.5\rho u_b^2$ ) | |
| $C_p$ | Specific heat at constant pressure | J / kg .$^o$C |
| $D_h$ | Hydraulic diameter | m |
| G | Generation term | kg / m. s$^3$ |
| h | Heat transfer coefficient | w / m .$^o$C |
| K | Von Karman constant | |
| L | Length of tube | m |
| m | Nodes number in z-direction | |

| | | |
|---|---|---|
| $\dot{m}$ | Mass flow rate | kg/s |
| n | Nodes number in r-direction | |
| Nu | Nusselts number (= $hD_h / \lambda$ ) | |
| $P$ | Perimeter | |
| P | Pressure | $N/m^2$ |
| $P_r$ | Prandtle number | |
| Q | Heat flux | $w/m^2$ |
| r | Radial dimension | |
| Re | Reynolds number (= $U_{in}D_h/\mu$) | |
| $R^*$ | Dimensionless radial distance( = r/R ) | |
| $v$ | Radial velocity | m/sec |
| T | Temperature | $^oC$ |
| u | Axial velocity | m/s |
| $u_b$ | Axial Bulk velocity | m/s |
| y | Dimensionless distance from the wall | |
| z | Axial Cartesian coordinate | m |
| $Z^*$ | Dimensionless axial length ( =z/D) | |

Greek Symbols

| | | |
|---|---|---|
| $\gamma$ | Coefficient of relaxation | |
| $\Omega$ | Velocity ratio (= $v_w /U_{in}$) | |
| $\varepsilon$ | Dissipation rate of turbulent kinetic energy | $m^2/s^3$ |
| k | Turbulent kinetic energy | $m^2/s^2$ |
| $\lambda$ | Fluid thermal conductivity | $W/m.^oC$ |
| $\mu$ | Viscosity | kg/m. s |
| $\theta$ | Dimensionless temperature | |
| $\upsilon_t$ | Kinematic turbulent viscosity | m / s |
| $\rho$ | Fluid density | $kg /m^3$ |
| $\sigma_\kappa$, $\sigma_\varepsilon$ | Turbulent Prandtle number | |
| $\Re$ | Gas Constant | J/kg.K |
| $\tau_w$ | Wall shear stress | $N /m^2$ |
| $\Psi$ | Fractional mass extraction (= $\dot{m}_w / \dot{m}_{in}$) | |

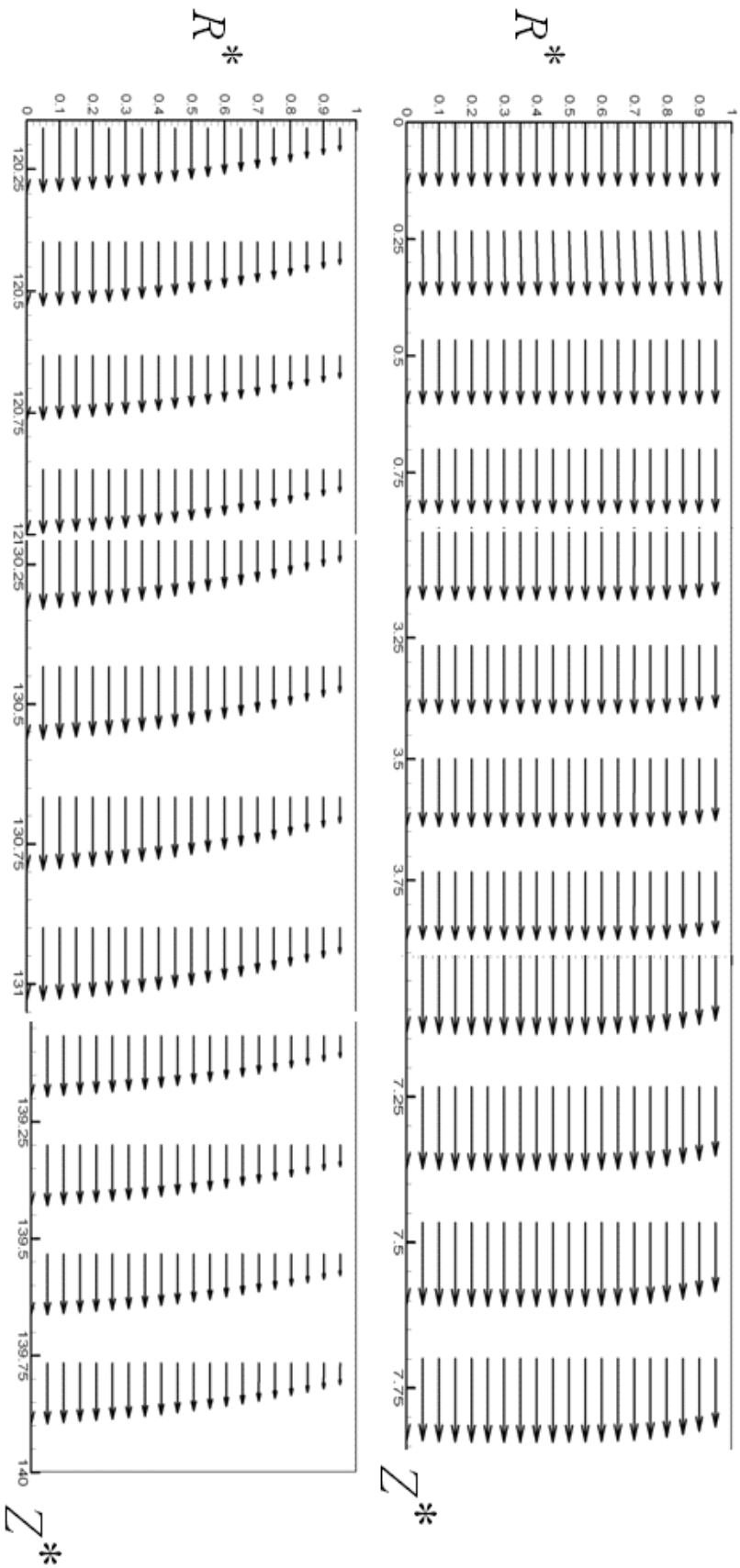


Fig(1).Developing Hydrodynamic Boundary Layer in Circular Tube for Flow with Constant Heat Flux at Re=1.78E+06(solid wall)

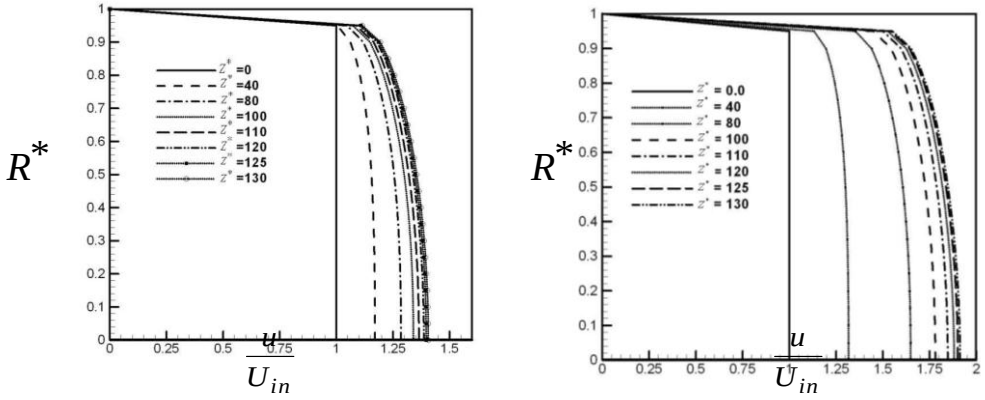


**(a). Constant Wall Temperature.** **(b). Constant Heat Flux.**

**Fig.2 : Developing Axial Velocity for Solid Wall**

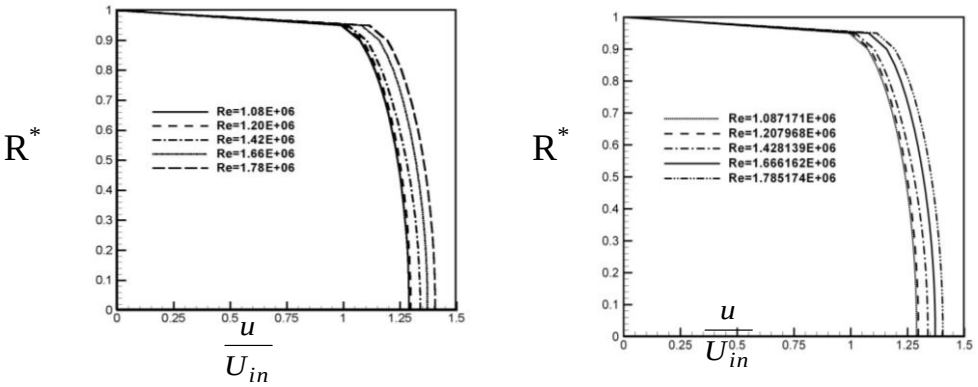


**(a). Constant Wall Temperature.** **(b). Constant Heat Flux.**

**Fig.3: Effect of Reynolds Number on Developing Velocity**

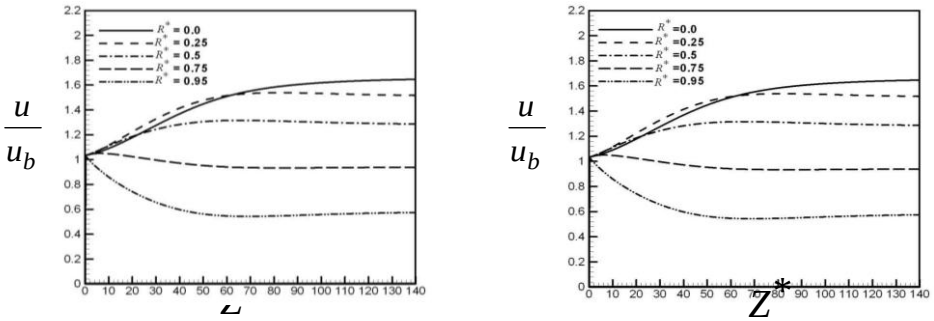


**(a). Constant Wall Temperature.** **(b). Constant Heat Flux.**

**Fig.4: Developing Axial Velocity for Solid Wall**

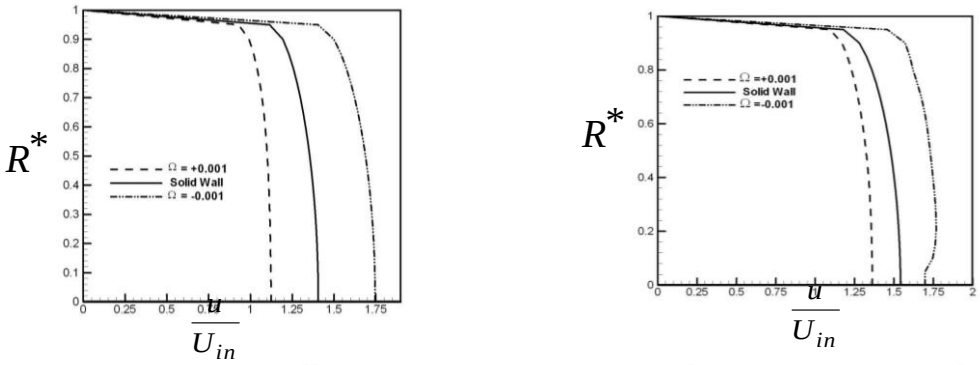


**(a). Constant Wall Temperature.** **(b). Constant Heat Flux.**

**Fig.5: Effect of Suction and Injection on Developing Axial Velocity**

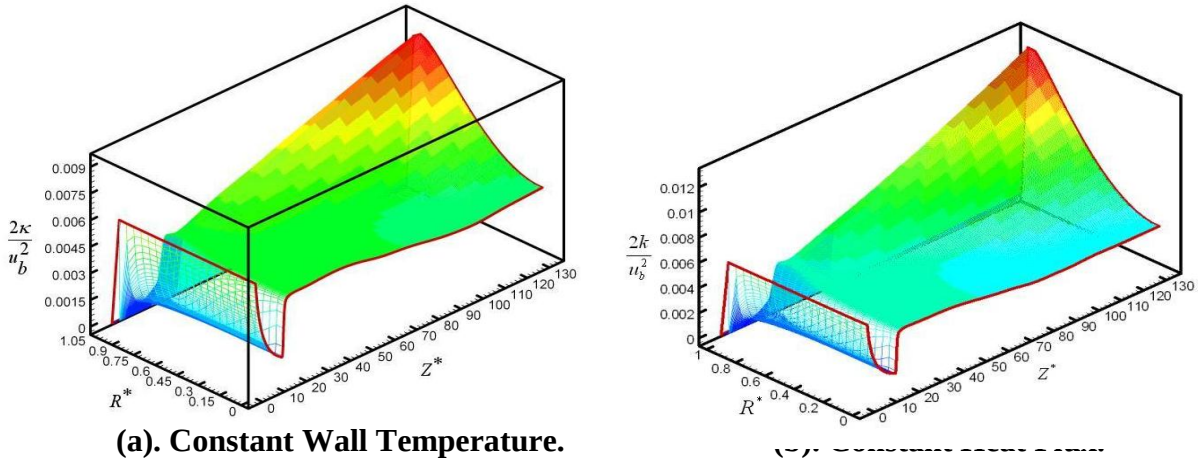


**(a). Constant Wall Temperature.**

**Fig.6: Development of Turbulent Kinetic Energy.**

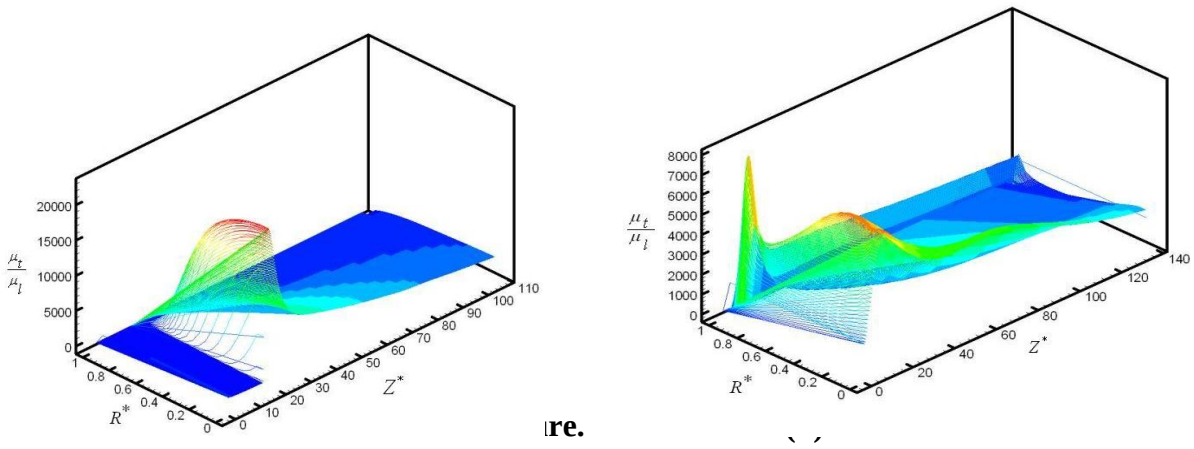


**re.**

**Fig.7: Development of turbulent viscosity for flow with**

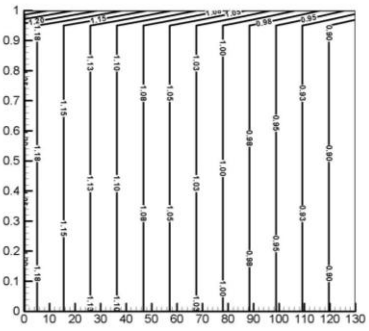

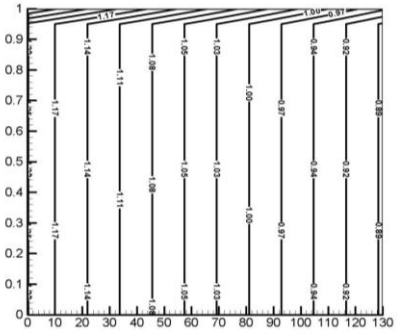

$R^*$

$Z^*$

**(a). Constant Wall Temperature.** **(b). Constant Heat Flux.**

**Fig.8: Developing Air Density for Flow with Re=1.78E+06**

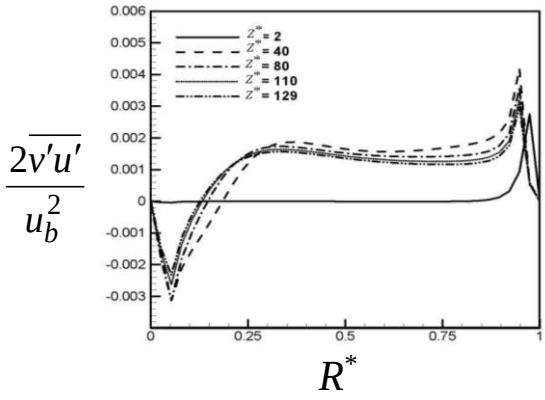


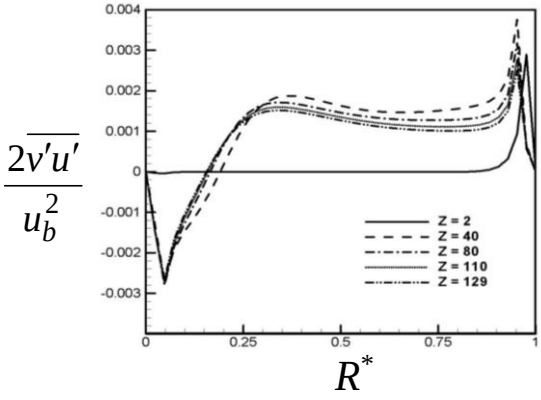


**(a). Constant Wall Temperature.** **(b). Constant Heat Flux.**

**Fig.9: Developing Reynolds Stress for Reynolds Number Re=3.57E+06.**

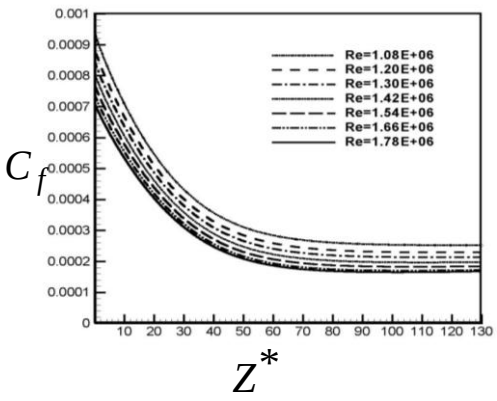


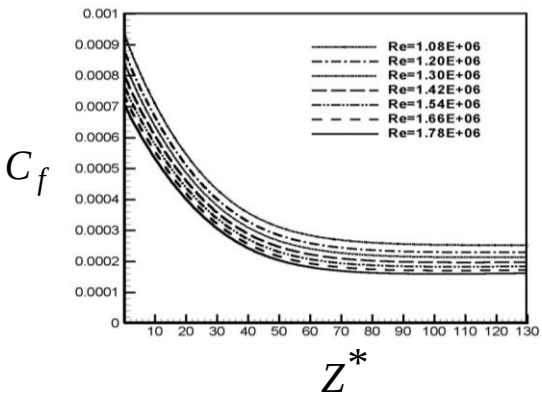

**(a). Constant Wall Temperature.** **(b). Constant Heat Flux.**

**Fig.10: Effect of Reynolds Number on the Local Coefficient of Friction**

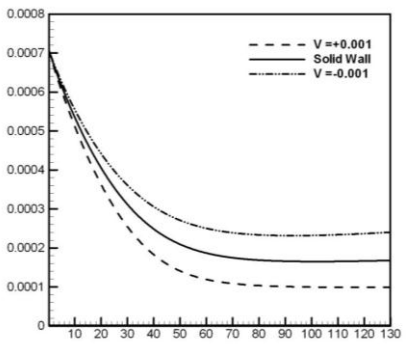


$C_f$

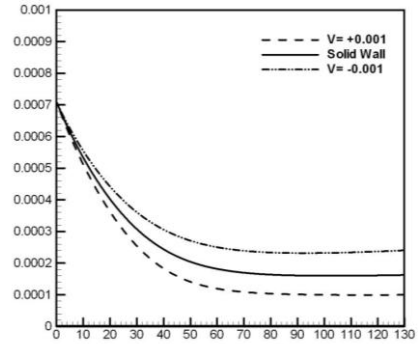


$C_f$

$Z^*$

**(a). Constant Wall Temperature.** **(b). Constant Heat Flux.**

**Fig.11: Effect of Suction and Injection on Local Coefficient of Friction.**

$Z^*$ $Z^*$

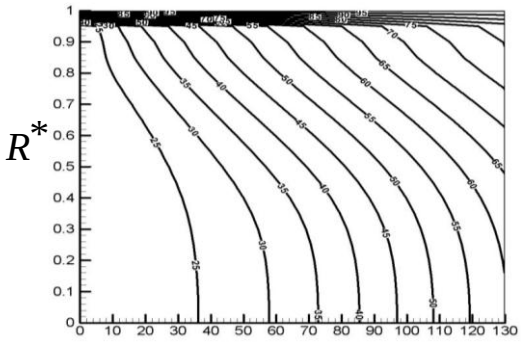

$R^*$

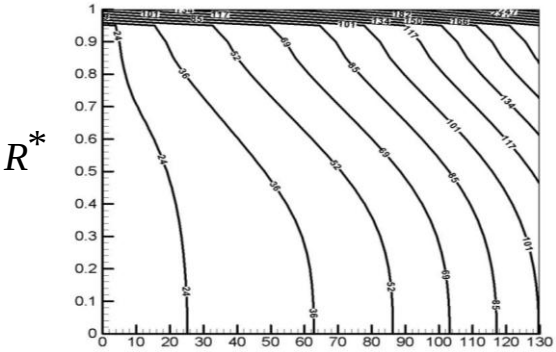

$R^*$

$Z^*$

**(a). Constant Wall Temperature.** **(b). Constant Heat Flux.**

**Fig.12: Isothermal Lines at Re=1.78E+06 .**

$\frac{T_b - T_{in}}{T_w - T_{in}}$

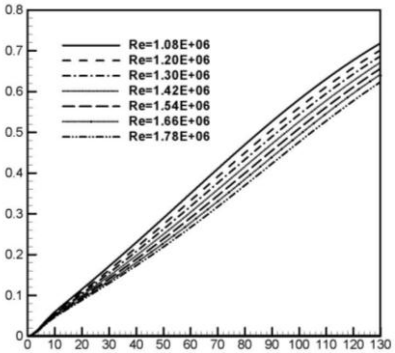


$Z^*$

$\theta_w$

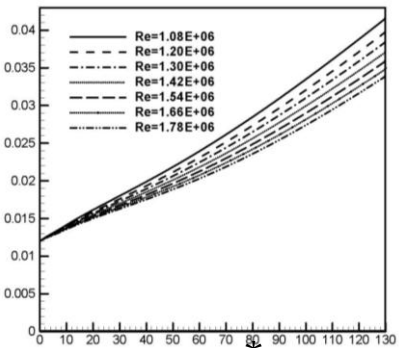


$Z^*$

**(a). Overall Heating.** **(b). Wall Temperature.**

**Fig.13: Effect of Reynolds Number on Overall Heating and Wall**

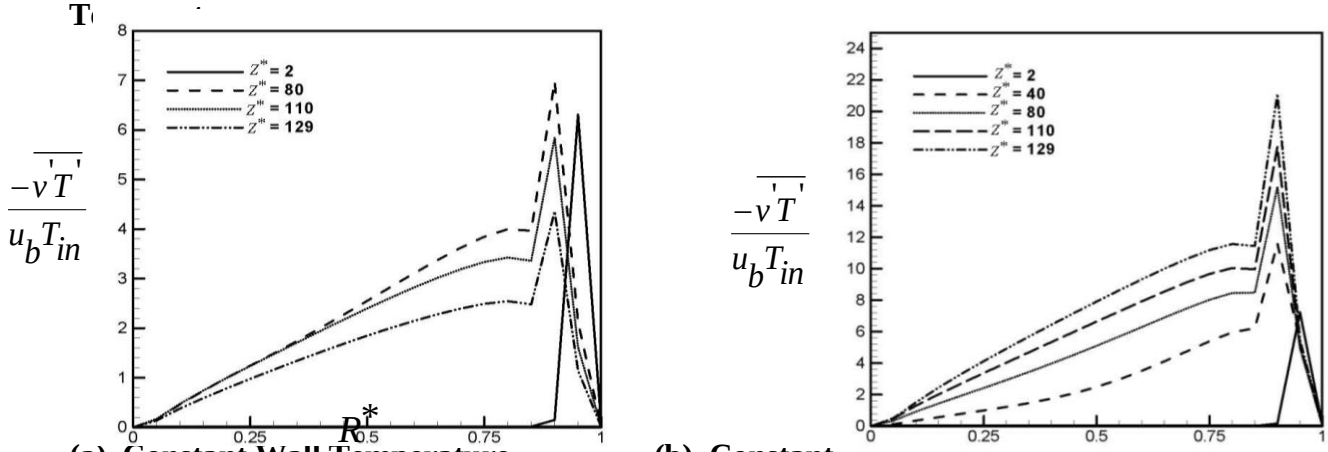


**(a). Constant Wall Temperature.** **(b). Constant Heat Flux.**

**Fig.15: Turbulent Heat Flux Developing Curve .**

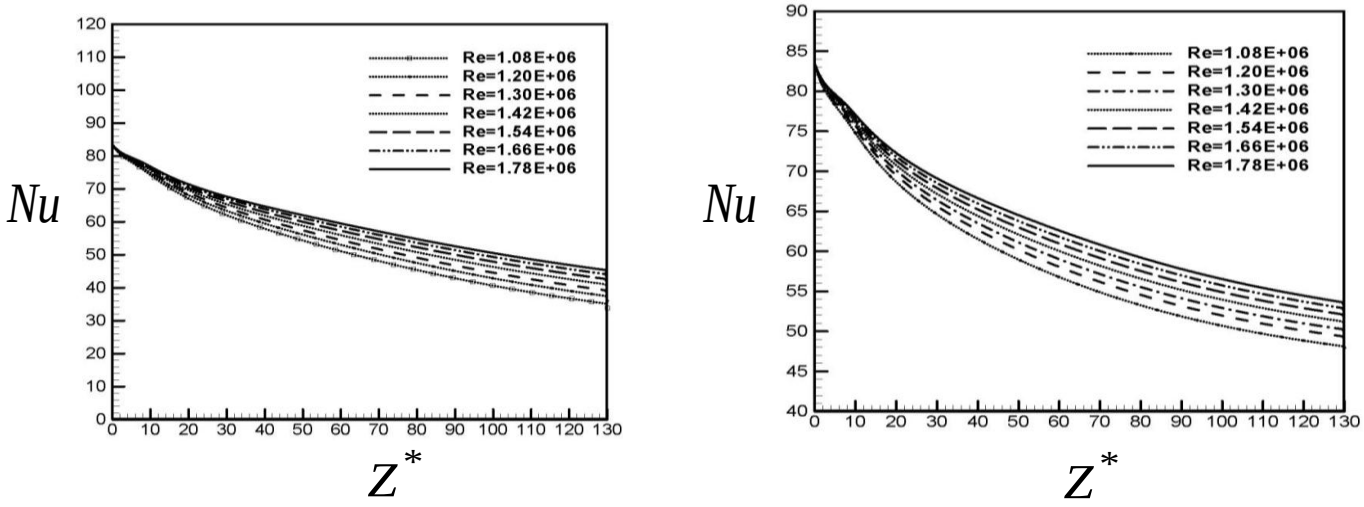


**(a). Constant Wall Temperature.** **(b). Constant Heat Flux.**

**Fig.16: Effect of Reynolds Number on Local Nusselt Number .**

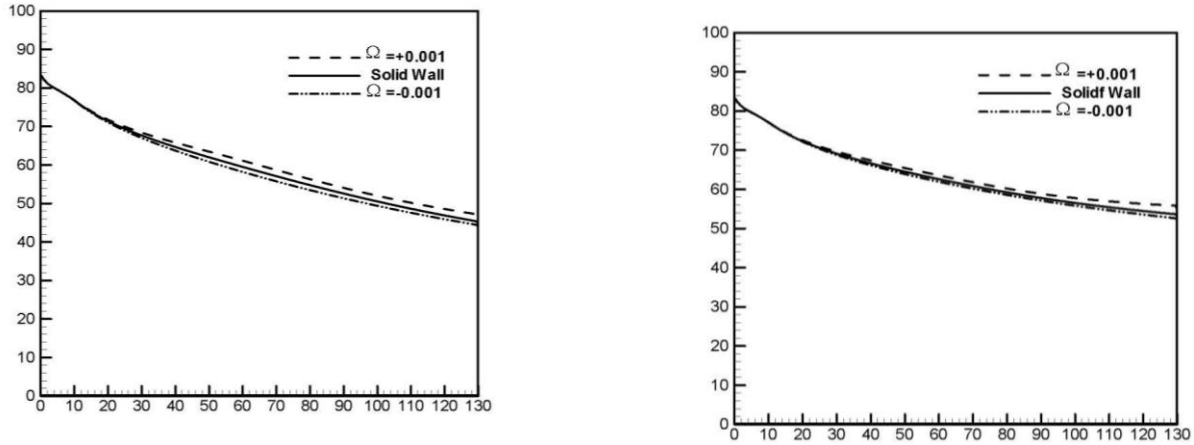

$Nu$ $Z^*$ $Nu$ $Z^*$

**(a). Constant Wall Temperature.** **(b). Constant Heat Flux.**

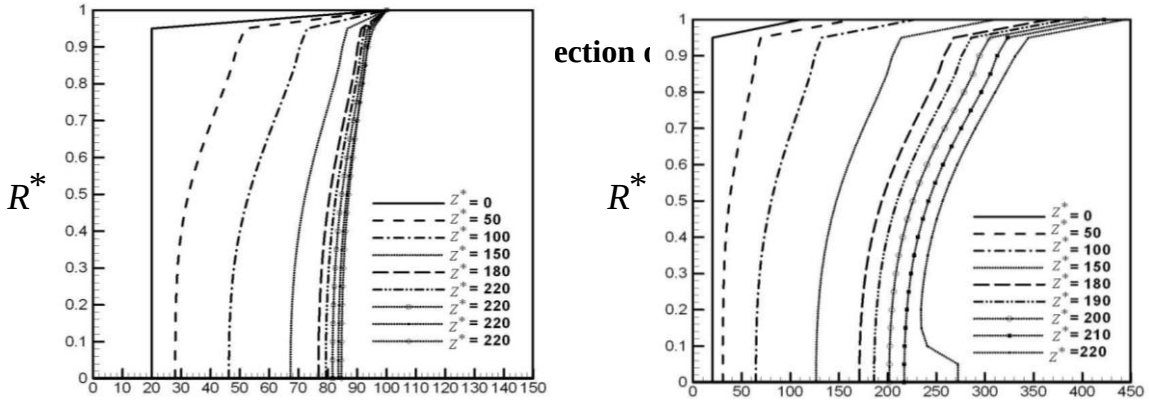


**ection (**

**(a). Constant wall temperature**. **(b). Constant heat flux.**

**Fig.18: Radial Temperature Developing Profile for Solid Wall**

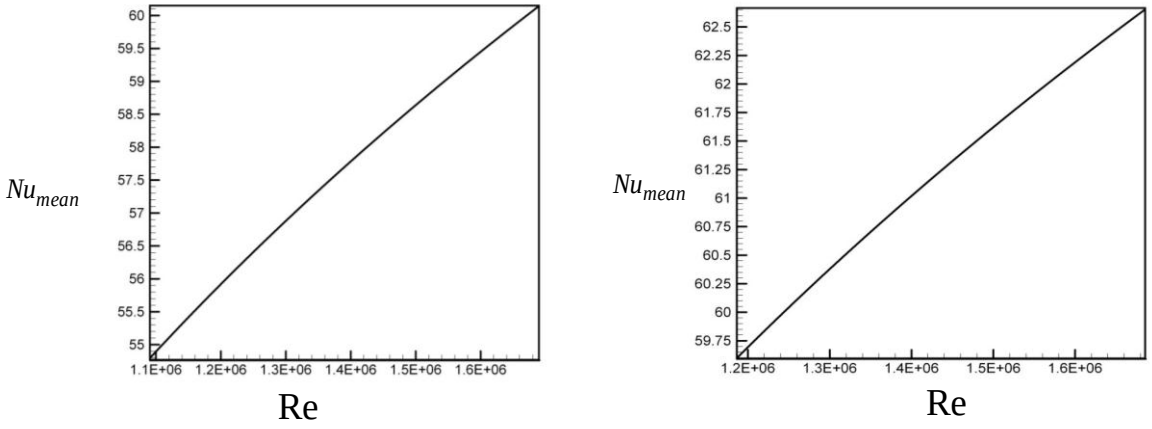


**(a). Constant wall temperature**. **(b). Constant heat flux.**

**Fig.19: The Relation Between Mean Nusselt Number and Rynolds Number**

$\frac{u}{u_b}$ $\frac{u}{u_b}$

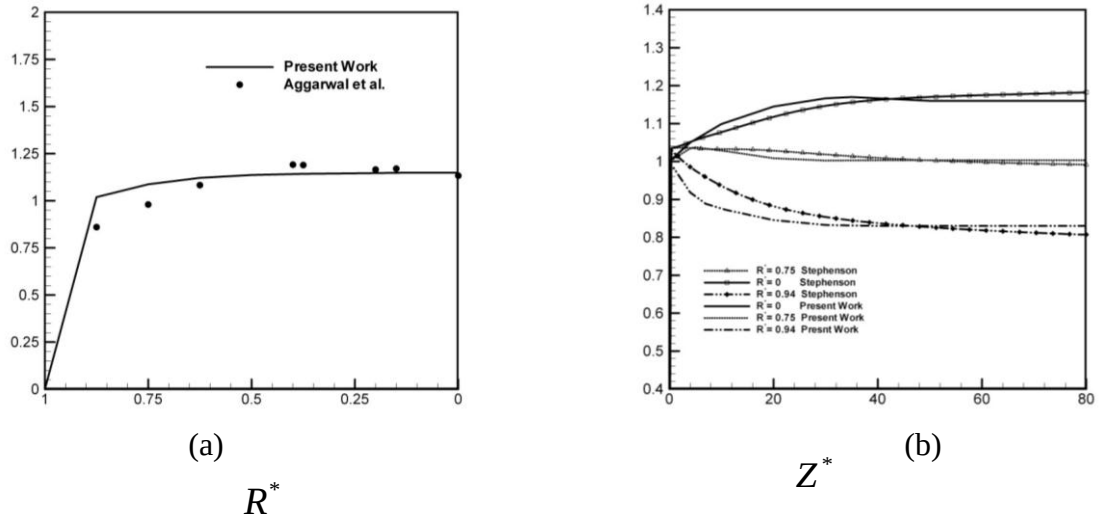


(a) (b)

$R^*$ $Z^*$

**Fig.20: Comparison Between the Present Work and Past Works**